



SNS EXTRACTION KICKER MAGNET WITH LOW $-\mu$ FERRITE

BNL/SNS TECHNICAL NOTE

NO. 109

H. Hahn and D. Davino

June 28, 2002

COLLIDER-ACCELERATOR DEPARTMENT
SNS PROJECT
BROOKHAVEN NATIONAL LABORATORY
UPTON, NEW YORK 11973

SNS EXTRACTION KICKER MAGNET WITH LOW- μ FERRITE

H. Hahn and D. Davino, Brookhaven National Laboratory, Upton, NY 11973 USA

Abstract

Kicker magnets typically represent the most important contributors to the transverse impedance budget of accelerators and storage rings. Methods of reducing the impedance value, a topic critical to the SNS extraction kicker presently under construction but also important in view of their possible application to other machines, have been thoroughly studied at this laboratory. In this report, the investigation of a potential improvement from using ferrite different from the BNL standard CMD5005 is reported. Permeability measurements of several ferrite types have been performed. Measurements on the full and half size SNS kicker prototype using CMD5005 and C2050 suggest that the impedance of a magnet with external resistive load is essentially unchanged. However, kickers without external resistive damping would benefit from the use of a low- μ ferrite.

I. Introduction

The transverse impedance of kicker magnets represent in typical collider accelerator or storage rings the largest single contributing element. Minimizing their impedance is obviously one of the major design objectives. Achieving the design performance of the Spallation Neutron Source (SNS) Accumulator Ring is expected to depend largely on achieving sufficiently reduced extraction kicker impedance [1]. Of particular concern is the impedance at the low frequency end with focus on frequencies below 100 MHz. Exhaustive impedance reduction studies involving a resistive termination are believed to have resulted in a satisfactory solution [2].

Another method, suggested by Danilov et al. [3] involved the use of low- μ ferrite. Their estimates indicated a reduced impedance peak and a shift to higher frequencies which would be advantageous for beam stability. The method of reducing the coupling impedance of kicker magnets by way of ferrite material with different properties was investigated in great detail and the results represent the topic of this report.

The "standard" ferrite material for kickers at this laboratory is CMD5005 from Ceramic Magnetics [4]. The company provided several samples of Ni-Zn Ferrites with different material properties. Their measurement confirmed the low losses associated with low permeability. Under the assumption that a $\mu < 100$ does not provide the required field quality, full size blocks of C2050 material for the kicker prototype were ordered. Comparative impedance measurements could thus be made using the same vacuum vessel and other hardware. In fact, the measurements were carried out on the full-size as well as a half-size version of the prototype. System measurements including the PFN-pulser were only done on the full size magnet and showed no significant differences when properly matched. No ferrite heating was observed on CMD5005 at nominal design operation.

The SNS extraction kicker is powered from a PFN pulser providing a 25Ω termination in order to achieve the rise time of ~ 200 ns as required. The impedance measurements indicated that any

potential impedance reduction due to the low- μ ferrite is effectively hidden under the termination. Consequently, without apparent improvement, the standard CMD5005 remains the obvious choice.

In contrast to the SNS extraction kicker, the RHIC abort kicker [5] is not terminated, and the transverse coupling impedance shows a distinct peak [6]. Judging from the results below, a significant impedance reduction with a lower loss material, such as CMD10, can be expected, although further R&D is indicated.

II. TRANSVERSE IMPEDANCE

The SNS extraction kickers are window frame magnets for vertical deflection of the beam. The prototype model has an aperture of ~ 24.6 cm vertically and ~ 15.9 cm horizontally. The ferrite comes as 31.8 mm thick bricks, each being roughly square with ~ 18 cm sides. The magnet is assembled with two bricks vertically, separated by copper stripes (a.k.a eddy current stripes) serving for longitudinal impedance reduction. The magnet has two bricks longitudinally for a ~ 36 cm ferrite length and a bus bar of 40 cm.

Transverse impedance measurements on the SNS kickers were made using the standard method [7], in which a twin-wire "Lecher" line is inserted into the kicker. The forward transmission coefficients of the "Device Under Test" and of a reference line of at least equal length is interpreted according to

$$Z_{\perp} = \frac{cZ^{DUT}}{\omega\Delta^2} = -2 \frac{cZ_L}{\omega\Delta^2} \ln \left(S_{21}^{DUT} / S_{21}^{REF} \right),$$

with $\Delta \approx 41$ mm being the spacing of the wires and $Z_L \approx 260 \Omega$ the characteristic impedance of the line, home-made from 5×7.5 mm tubes. Matching of the line impedance to the 50Ω is achieved by means of a transformer (North Hills 0501BB) with a center-tapped secondary winding serving as 180° hybrid together with matching resistors. The measurements were made with the network analyzer, Agilent 8753ES, set for a logarithmic frequency range from 100 kHz to 100 MHz, 1601 points, and a 100 Hz bandwidth.

Vertical Impedance

The transverse impedance measurements were performed on the full-size SNS extraction kicker prototype as well as a half-size version thereof. The vertical coupling impedance for the prototype assembled with CMD5005 and C2050 ferrite bricks is compared in Fig. 1 for the half-size model and in Fig. 2 for the full-size model.

The results, appropriately scaled, are in qualitative agreement. This fact is noted in order to eliminate an interpretation of the result as due to size-dependent effects. The small difference between full-size and half-size, in particular the clean resonance curve in the half-size, is attributed to the absence of the copper stripes in the half-size model.

The figures point to certain differences between the actual results and the expectations. First, the resonance frequency is not upward shifted, indicating that the magnet inductance is essentially μ -independent and determined by the horizontal aperture dimension.

Second, although the nominally low-loss C2050 ferrite in fact yields a lower resonance peak, the CMD5005 has a sharper "high-Q" resonance. In theory, this type of behavior can be attributed to the skin effect in ferrite

$$\delta_{\mu}^{-1} \approx \omega \sqrt{\mu \left(\varepsilon - j \frac{\sigma}{\omega} \right)}$$

but in the frequency range considered here, the DC conductivity, σ , can be neglected and the magnetic properties of the unit are only determined by the ferrite permeability.

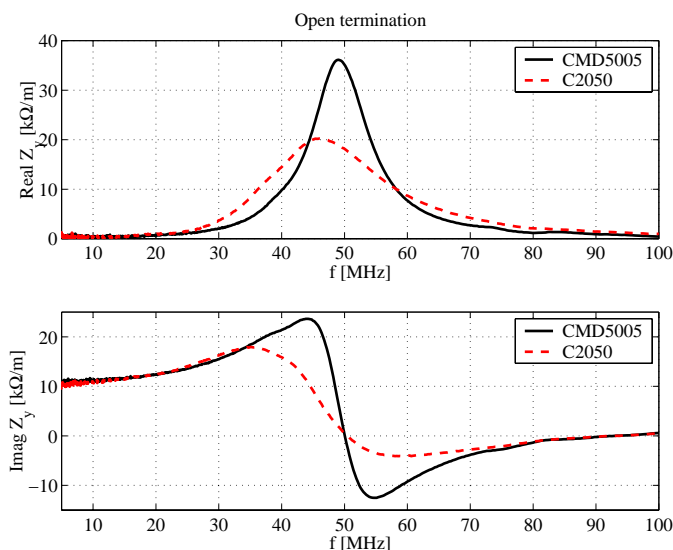


Fig. 1: Vertical impedance of half-size prototype

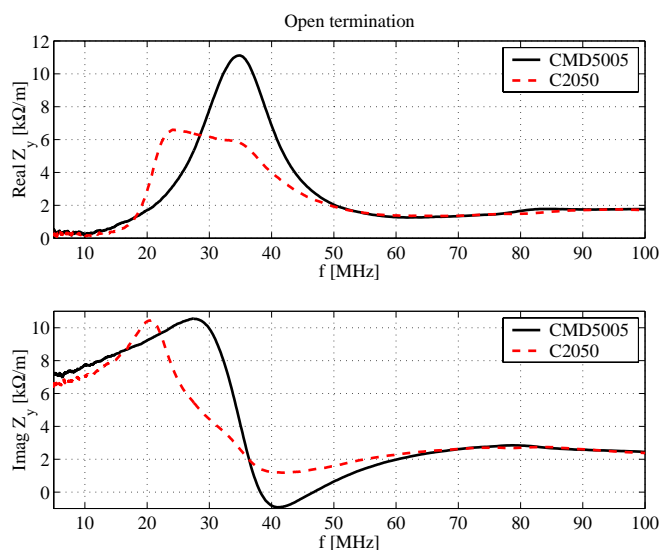


Fig. 2: Vertical impedance of full-size prototype

The ferrite measurements described in the next section of this paper led to an interpretation of the observations based on the concept of sheared/effective permeability [8]

$$\mu_{eff} = \mu_0 \frac{\mu' - j\mu''}{1 + N(\mu' - j\mu'')}$$

where N is the fraction of the air gap in the magnetic circuit. In the case of high- μ material, the effective permeability at low frequencies is approximately

$$\mu_{eff} \approx \mu_0 \left\{ \frac{\mu'}{1 + N\mu'} - j \frac{\mu''}{(1 + N\mu')^2} \right\}$$

It follows that the inductance is essentially independent of μ' and explains the unchanged resonance frequency. The losses are reduced, quadratically with the permeability, which leads to a larger quality factor and sharper resonance in the high- μ material. The concept of sheared permeability due to the air gap is in qualitative agreement with observations and is considered as their probable interpretation.

Horizontal Impedance

The horizontal coupling impedance measured on the full-size prototype for both ferrite materials is shown in Fig. 3. The impedance of the half-size magnet, shown in Fig.4, is insignificantly lower. The magnetic field here does not couple into the external bus bar circuit and the resonance is absent. In the full-size magnet, the magnetic circuit is interrupted by the lateral copper stripes, which leads to low horizontal impedance values. Note that the low-loss C2050 ferrite yields only slightly lower impedance value, pointing to the presence of the shearing effect.

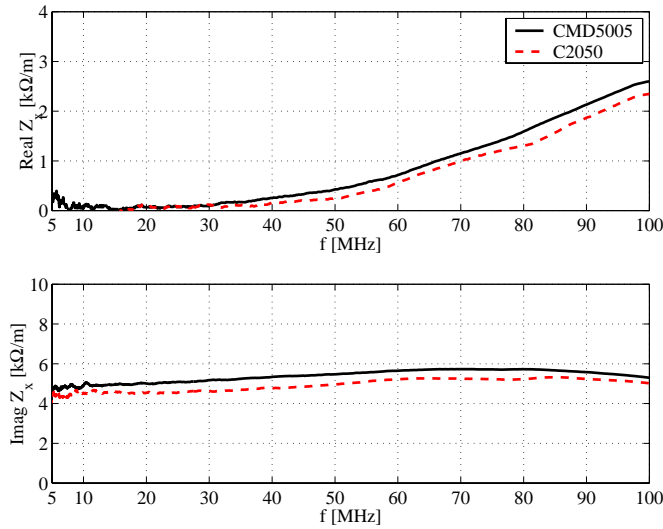


Fig. 3: Horizontal impedance of full-size prototype

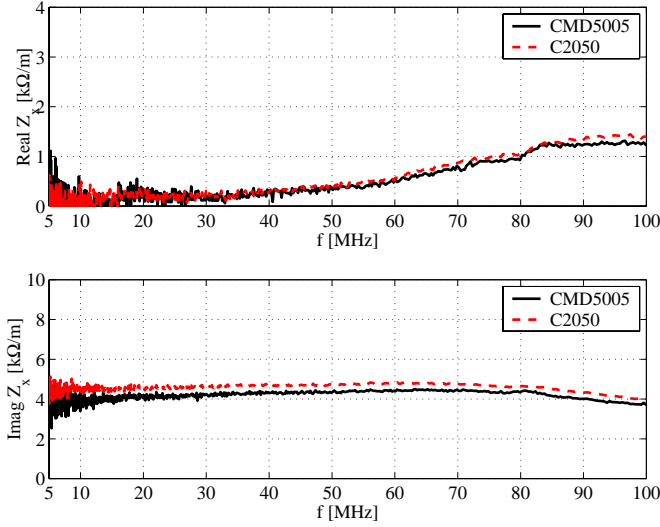


Fig. 4: Horizontal impedance of half-size prototype

III. FERRITE MEASUREMENTS

Toroidal sample measurements

Several toroidal samples of ferrite material with different permeability, including C2050, CMD10 and N40, were obtained by courtesy of Ceramic Magnetics. The rings were wound with a 10 turn coil and terminated into a BNC connector. The coil inductance is given by

$$L = \mu n^2 \frac{t}{2\pi} \ln \frac{b}{a}$$

with $b = 13.7$ mm, $a = 7.9$ mm, $t = 3.6$ mm and $n = 10$, leading to $L = 40$ nH.

The input impedance was measured from 0.1 to 100 MHz with the network analyzer. The results for the materials used in the magnet as well as a Rexolite ring of identical geometry are shown in Fig. 5. The ferrite rings exhibit a resonance due to the ~ 5.6 pF capacity of the BNC connector. The Rexolite ring has a resonance outside the measured range and shows an inductance of ~ 0.24 μ H, a value 6-times larger than the formula.

The inductance of the ferrite rings is obtained by subtracting the capacitive resonance contribution. The permeability of the ferrite is then given by the ratio of ferrite over the theoretical or measured reference inductance. The results can be presented by the expression [9]

$$\mu' - j\omega\mu'' = \frac{\mu_i - 1}{1 + j\omega / \omega_s}$$

with the initial permeability, μ_i , and the saturation frequency, ω_s . The measured values clearly show the lower losses of the "low- μ " ferrite, but differ in the initial permeability values quoted by the manufacturer. Combining all data results in the parameters for the ferrites

CMD5005: $\mu_i = 1600$, $\omega_s = 2.7$ MHz
 C2050: $\mu_i = 100$, $\omega_s = 55$ MHz

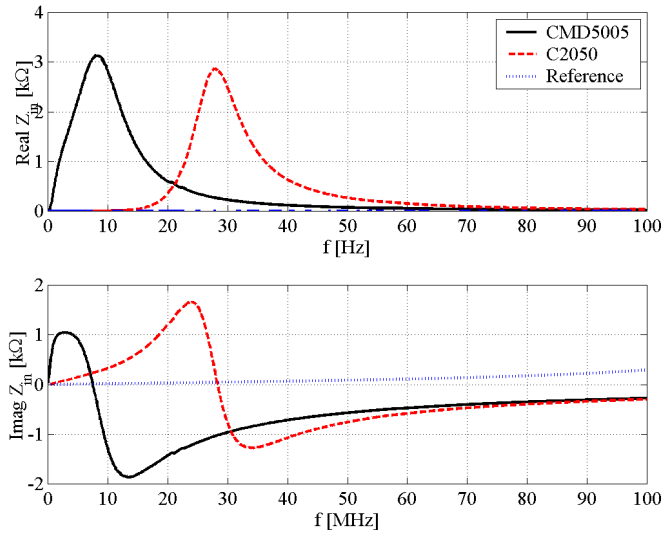


Fig. 5: Input impedance of ferrite and reference rings

Ferrite Brick Measurements

With the goal of investigating any size dependent effects, a closed magnetic circuit was arranged with two large bricks from the kicker magnet, 18'18'3 cm, separated by small blocks, 7'5'1.4 cm, and driven with a 10 turn winding. The input impedance was obtained for the two ferrite materials and is shown in Fig. 6. The resonance curves are similar to those in the sample rings, although the ratio of the resonance frequencies is ~ 2.8 for the bricks versus ~ 3.5 for the rings, and is lower than the ratio 4, expected from the initial permeabilities. These ratios could point to a size effect due to the factor 100 difference in the DC resistivity of the ferrites

The most plausible interpretation of the changes in coupling impedance with the ferrite material seems to be the shearing effect. This was directly confirmed by placing a 10 turn winding on a single large brick. Its input impedance is given in Fig. 7 showing a qualitative agreement with the input impedance at the kicker bus bar. Note the overlapping resonances with high-Q for the high- μ CMD5005 and the lower Q for the low- μ C2050 ferrite.

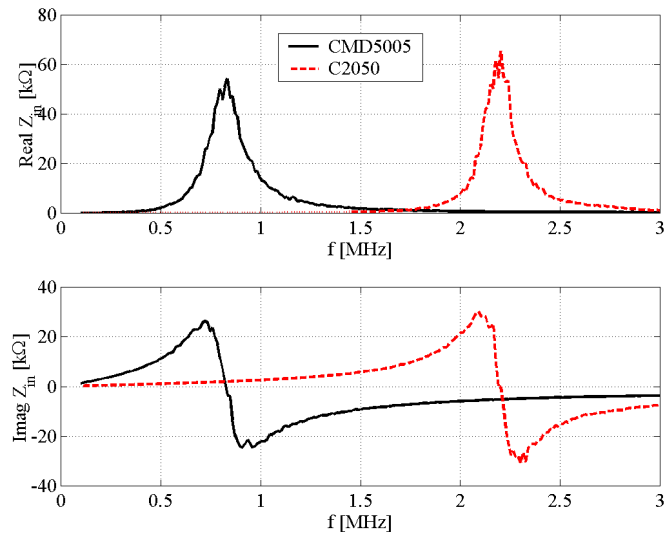


Fig. 6: Input impedance of a coil on the two-brick arrangement

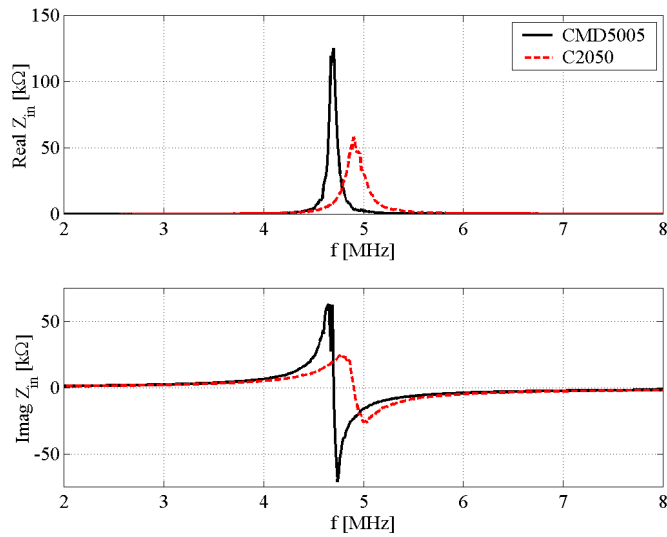


Fig. 7: Input impedance of a coil on a single brick

Acknowledgements

The authors would like to thank Chen-Ih Pai for mechanical engineering contributions and the Beam Components Group and the Pulsed Power Group of the Collider-Accelerator Department for technical support.

References

- [1] J. Wei et al., EPAC2002, Paris, paper THPLE014.
- [2] D. Davino, H. Hahn, and Y-Y. Lee, EPAC2002, Paris, paper WEPR036.
- [3] V. Danilov, S. Kurennoy and M. Blaskiewicz (unpublished).
- [4] G. E. Schaller, Ceramic Magnetics, Inc., 16 Law Drive, Fairfield, NJ 07004 (973-227-4222).
- [5] H. Hahn, A. Dunbar, C. I. Pai, R. T. Sanders, N. Tsoupas, and J. E. Tuozzolo, Proc. 1999 Pac, New York, p. 1100.
- [6] H. Hahn and D. Davino, Proc. 2001 PAC, Chicago, IL p. 1829.
- [7] F. Caspers in Handbook of Accelerator Physics and Engineering, ed. A.W. Chao and M. Tigner (World Scientific, Singapore 1998) p. 571.
- [8] H.P.J. Wijn and P. Dullenkopf, Werkstoffe der Elektrotechnik, (Springer-Verlag, Berlin 1967) p. 90.
- [9] L. Vos, report CERN-SL-2000-010 AP (March 2000).